Appl Microbiol Biotechnol (2013) 97:195–203
DOI 10.1007/s00253-012-4074-4

BIOTECHNOLOGICALLY RELEVANT ENZYMES AND PROTEINS

A comparison of two novel alcohol dehydrogenase enzymes (ADH1 and ADH2) from the extreme halophile *Haloferax volcanii*

Leanne M. Timpson · Ann-Kathrin Liliensiek · Diya Alsafadi · Jennifer Cassidy · Michael A. Sharkey · Susan Liddell · Thorsten Allers · Francesca Paradisi

Received: 2 March 2012 / Revised: 28 March 2012 / Accepted: 31 March 2012 / Published online: 25 April 2012

Abstract Haloarchaeal alcohol dehydrogenases are exciting biocatalysts with potential industrial applications. In this study, two alcohol dehydrogenase enzymes from the extremely halophilic archaeon *Haloferax volcanii* (*Hv*ADH1 and *Hv*ADH2) were homologously expressed and subsequently purified by immobilized metal-affinity chromatography. The proteins appeared to copurify with endogenous alcohol dehydrogenases, and a double Δ*adh2* Δ*adh1* gene deletion strain was constructed to prevent this occurrence. Purified *Hv*ADH1 and *Hv*ADH2 were compared in terms of stability and enzymatic activity over a range of pH values, salt concentrations, and temperatures. Both enzymes were haloalkaliphilic and thermoactive for the oxidative reaction and catalyzed the reductive reaction at a slightly acidic pH. While the NAD^+-dependent *Hv*ADH1 showed a preference for short-chain alcohols and was inherently unstable, *Hv*ADH2 exhibited dual cofactor specificity, accepted a broad range of substrates, and, with respect to *Hv*ADH1, was remarkably stable. Furthermore, *Hv*ADH2 exhibited tolerance to organic solvents. *Hv*ADH2 therefore displays much greater potential as an industrially useful biocatalyst than *Hv*ADH1.

Keywords Alcohol dehydrogenase · Biocatalyst discovery · Protein characterization · Extremophile · *Haloferax volcanii* · Organic solvents

L. M. Timpson and A.-K. Liliensiek contributed equally to this work.

L. M. Timpson · A.-K. Liliensiek · D. Alsafadi · J. Cassidy · F. Paradisi (✉)
Centre for Synthesis and Chemical Biology,
UCD School of Chemistry and Chemical Biology,
University College Dublin,
Belfield, Dublin 4, Ireland
e-mail: francesca.paradisi@ucd.ie

M. A. Sharkey
UCD School of Biomolecular and Biomedical Science,
Conway Institute, University College Dublin,
Belfield, Dublin 4, Ireland

S. Liddell
Division of Animal Sciences, School of Biosciences,
University of Nottingham,
Sutton Bonington Campus,
Loughborough LE12 5RD, UK

T. Allers (✉)
Institute of Genetics, School of Biology,
University of Nottingham, Queen's Medical Centre,
Nottingham NG7 2UH, UK
e-mail: thorsten.allers@nottingham.ac.uk

Introduction

Alcohol dehydrogenases (ADHs, EC 1.1.1.1), an important group of biocatalysts that catalyze the interconversion between alcohols and aldehydes and ketones, are attracting significant biotechnological interest (Eichler 2001; Parkot et al. 2010). They find a range of applications in biosensor-based diagnostics and in fuel cell technology (Yakushi and Matsushita 2010) and, particularly, in the stereo-specific production of industrially valuable chiral alcohols (Goldberg et al. 2007). Additionally, ADHs can accomplish dynamic kinetic resolution processes by which high yields (theoretically up to 100 %) of a single enantiomer can be obtained. Such processes are attractive to the pharmaceutical industry for the production of enantiopure chemical entities and products (Friest et al. 2010; Giacomini et al. 2007).

The application of mesophilic enzymes as industrial biocatalysts is constrained to narrow operating ranges of temperature, pH, and pressure. One approach to tackle the

incompatibility between industrial conditions and biological components (Danson and Hough 1998; Hough and Danson 1999) is to employ enzymes from extremophiles, which exhibit tolerance to a range of environmental stressors (Adams et al. 1995). The majority of *extremozymes*, and ADHs, reported to date have been thermophilic, leaving the biotechnological potential of haloarchaeal extremozymes relatively unexplored (Eichler 2001).

Haloarchaeal proteins are adapted to remain soluble, stable, and catalytically active at high ionic strength (Coquelle et al. 2010; Oren 2002), and, as a result of comparisons drawn between hypersaline and organic solvent environments (Flam 1994), halo-adapted proteins have been reported to tolerate organic cosolvents to a greater degree than their mesophilic counterparts (Timpson et al. 2012).

For their biotechnological application to be realized, methods for the efficient production and purification of haloarchaeal proteins are essential (Connaris et al. 1999). While *Escherichia coli* is an industrially attractive host (Baneyx 1999), which has been successfully employed for the overexpression of several haloarchaeal proteins (Cendrin et al. 1993; Connaris et al. 1999), a frequent consequence of their expression in a low ionic strength internal environment is the formation of inclusion bodies, necessitating solubilization and refolding procedures (Singh and Panda 2005). This provides incitement for protein expression in a halophilic host, in which the direct production of soluble, active protein is highly probable.

We recently reported on the production and characterization of an ADH from *Haloarcula marismortui* (*Hm*ADH12) (Timpson et al. 2012). Now, in a continuous effort to identify other novel haloarchaeal ADHs with potential biotechnological applications, we describe the homologous overexpression and purification of two ADHs from *Haloferax volcanii* (*Hv*ADH1 and *Hv*ADH2), using a native expression system (Allers et al. 2010). The identification and the biochemical characterization of both enzymes are reported. The effect of organic solvents on the activity of *Hv*ADH2 and the requirement for high salt concentration is also explored.

Materials and methods

Reagents, strains, and culture conditions

All chemical reagents, unless stated otherwise, were purchased as analytical grade from Sigma-Aldrich. Restriction enzymes were purchased from New England Biolabs (USA). Standard molecular techniques were used. PCR amplification used Phusion™ DNA polymerase (Finnzymes). *H. volcanii* strains were grown at 45 °C on complete (*Hv*-YPC) or casamino acids (*Hv*-Ca) agar, or in *Hv*-YPC or *Hv*-Ca broth, as described previously (Guy et al. 2006). Isolation of genomic and plasmid DNA and transformation of *H. volcanii* were carried out as described previously (Allers et al. 2004; Norais et al. 2007).

Construction of expression plasmid pTA1202-*adh1*

The *H. volcanii adh1* gene (HVO_2428) was PCR amplified from genomic DNA using forward and reverse primers adh1F (5′-ACCTATTGCGCATATGCACCACCACCACCACCACATGAGAGCCGCAGTCCTCCG-3′) and adh1R (5′-CCGCCGAATTCCGATTTTACGGAACC-3′). The adh1F primer featured an *Nde*I site for cloning (underlined) and an in-frame $(CAC)_6$ tract for the 6xHis tag. The adh1R primer featured an *Eco*RI site for cloning (underlined). The 1,112-bp PCR product was digested with *Nde*I and *Eco*RI, ligated with pTA963 (also digested with *Nde*I and *Eco*RI), and used to transform *H. volcanii* H1209 (Δ*pyrE2* Δ*hdrB Nph-pitA* Δ*mrr*) directly (Allers et al. 2010). Plasmid DNA isolated from candidate clones was screened by *Nde*I/*Bam*HI restriction digest and verified by DNA sequencing. The *adh1* expression plasmid was designated pTA1202 and the pTA1202-harboring strain *H. volcanii* H1238.

Construction of expression plasmid pTA1205-*adh2*

The *H. volcanii adh2* gene (HVO_B0071) was PCR amplified from genomic DNA using forward and reverse primers adh2F (5′-CACAGCGTTCATGAAATCAGCAGTC-3′) and adh2R (5′-GTCTGGATCCGGGTGTGTCTTACTCG-3′). The adh2F primer features a *Bsp*HI site and the adh2R primer features a *Bam*HI site for cloning (both underlined). The 1,079 bp PCR product was digested with *Bsp*HI and *Bam*HI, ligated with pTA963 (digested with *Pci*I and *Bam*HI), and used to transform *H. volcanii* H1209 (Δ*pyrE2* Δ*hdrB Nph-pitA* Δ*mrr*) directly (Allers et al. 2010). Plasmid DNA isolated from candidate clones was screened by *Nde*I/*Bam*HI restriction digest and verified by DNA sequencing. The *adh2* expression plasmid was designated pTA1205 and the pTA1205-harboring strain *H. volcanii* H1239.

Construction and transformation of mutant *H. volcanii* strains

To generate the *adh2* deletion construct, pTA1230, a 1,228-bp region upstream of *adh2* was PCR amplified using primers dAdh2UF (5′-CCGGGGTACCTCCAGAAGACC-3′) and dAdh2UR (5′-GTTTCAGCGGATCCTATCCCCG-3′), and a 1,156-bp region downstream of *adh2* was amplified using dAdh2DF (5′-GCTGTGAGGATCCGACCTTGCG-3′) and

dAdh2DR (5′-CTCGTCTAGATCGACCAGCAC-3′). These PCR products were digested with *Bam*HI and ligated to each other. The resulting fragment was then digested with *Kpn*I and *Xba*I and ligated with pTA131 (also digested with *Kpn*I and *Xba*I). To generate the *adh1* deletion construct, pTA1229, a 971-bp region upstream of *adh1* was amplified using dAdh1UF (5′-GCCGTCATCGATCTCCAAGCC-3′) and dAdh1UR (5′-GGACTGCGGATCCCATACGCG-3′), and a 1,011-bp region downstream of *adh1* was amplified using dAdh1DF (5′-TCCGTAGGATCCGGGTTGGGCG-3′) and dAdh1DR (5′-ACGTCTAGAAGGGCGAAGTGTG-3′). These PCR products were digested with *Bam*HI and ligated to each other. The resulting fragment was then digested with *Cla*I and *Xba*I and ligated with pTA131 (also digested with *Cla*I and *Xba*I). All restriction sites used are underlined in the primers. *H. volcanii* Δ*adh* mutant strains were generated using a previously described gene knockout system (Allers et al. 2004; Bitan-Banin et al. 2003). *H. volcanii* H1209 was the source strain for generation of single Δ*adh2* and Δ*adh1* mutant strains. The resultant strains were designated *H. volcanii* H1290 (Δ*pyrE2* Δ*hdrB Nph-pitA* Δ*mrr* Δ*adh2*) and *H. volcanii* H1288 (Δ*pyrE2* Δ*hdrB Nph-pitA* Δ*mrr* Δ*adh1*). The strain *H. volcanii* H1290 was the source strain for the generation of a double gene deletion (Δ*adh2* Δ*adh1*) mutant strain. The resultant strain *H. volcanii* H1325 (Δ*pyrE2* Δ*hdrB Nph-pitA* Δ*mrr* Δ*adh2* Δ*adh1*) was transformed with pTA1202 and pTA1205. The double deletion mutant strains, harboring the pTA1202 and pTA1205 expression vectors, were designated *H. volcanii* H1330 and *H. volcanii* H1332, respectively.

Production and identification of *Hv*ADH1 and *Hv*ADH2

The expression, purification, and subsequent identification of *Hv*ADH1 and *Hv*ADH2 using ESI-Q-TOF2 tandem mass spectrometry was performed as described previously (Timpson et al. 2012).

Size exclusion chromatography

The molecular mass of the native *Hv*ADH1 and *Hv*ADH2 was determined as described previously (Timpson et al. 2012), but with buffers containing both 1 and 2 M NaCl.

Activity assays

Activity assays were performed as described previously (Timpson et al. 2012). The reaction mixture for the oxidative step routinely contained ethanol (100 mM), $NAD(P)^+$ (1 mM), enzyme sample (10 μL of suitable enzyme concentration), and 50 mM potassium phosphate, pH 11.0, containing KCl (3 M), when assaying *Hv*ADH1 activity, and 50 mM glycine-KOH, pH 10.0, containing KCl (4 M), when assaying *Hv*ADH2 activity. The reaction mixture for the reductive step routinely contained acetaldehyde (50 mM), NAD(P)H (0.1 mM), enzyme sample (10 μL of suitable enzyme concentration), and 50 mM citric acid–K_2HPO_4, pH 6.0, containing KCl (4 M) or KCl (1 M), when assaying *Hv*ADH1 or *Hv*ADH2 activity, respectively.

Characterization of *Hv*ADH1 and *Hv*ADH2

Oxidative reaction optima were determined by assaying *Hv*ADH1 and *Hv*ADH2 for activity against ethanol, 1-propanol, 1-butanol, 1-pentanol, 2-propanol, 2-butanol, isoamyl alcohol, and benzyl alcohol (100 mM) with $NAD(P)^+$ (1 mM) using the buffers: 50 mM sodium pyrophosphate, pH 8.0, containing 2–4 M KCl, 50 mM Tris–HCl, pH 8.0, containing 2–4 M NaCl, 50 mM glycine–KOH/NaOH, pH 9.0 and 10.0, containing 2–4 M KCl/NaCl, and 50 mM potassium/sodium phosphate, pH 11.0, containing 2–4 M KCl/NaCl. Reductive reaction optima were determined by assaying *Hv*ADH1 and *Hv*ADH2 for activity against acetaldehyde (50 mM) with NAD(P)H (0.1 mM) using the buffers: 50 mM citric acid–K_2HPO_4, pH 5.0 and 6.0, containing 2–4 M KCl and 50 mM potassium phosphate, pH 7.0, containing 2–4 M KCl. The optimum temperature for activity was determined by performing the standard assay for the oxidative reaction between 30 and 95 °C. The substrate specificity of *Hv*ADH1 and *Hv*ADH2 was investigated by screening for ADH activity against a range of alcohol substrates (100 mM) and the coenzyme dependency of the enzymes determined using both nicotinamide coenzymes (1 mM). *Hv*ADH1 was stored neat and with methanol [5–20 % (*v*/*v*)] at −20 °C. Samples (250 μL) of *Hv*ADH1 were also lyophilized and stored at −20 °C. Lyophilized *Hv*ADH1 was resuspended in the original volume of deionized water at regular intervals and assayed for preservation of activity. *Hv*ADH2 was stored neat and with glycerol [40 % (*v*/*v*)]. To investigate organic solvent tolerance, *Hv*ADH2, HLADH, and YADH were incubated for 24 h at 4 °C with 10 % (*v*/*v*) polar aprotic organic solvents dimethyl sulfoxide (DMSO), acetonitrile (ACN), and tetrahydrofuran. *Hv*ADH2 was subsequently incubated with 5, 10, and 30 % (*v*/*v*) DMSO, ACN, and methanol for 72 h at 4 °C in 100 mM Tris–HCl buffer, pH 8.0, containing KCl (2 M). The enzymes were assayed for activity at time zero and after incubation. HLADH and YADH were assayed in 100 mM sodium pyrophosphate buffer, pH 8.8, using NAD^+ (1 mM). For the determination of K_m and V_{max} values, initial rate measurements were performed at varying ethanol, $NAD(P)^+$, acetaldehyde, and NAD(P)H concentrations as described previously (Timpson et al. 2012). All measurements were performed in duplicate, and if the discrepancy between the results was >10 %, additional reactions were carried out.

The data were analyzed using SigmaPlot (Version 11.0), with nonlinear regression analysis (Wilkinson 1961).

Results

Expression of *Hv*ADH1 and *Hv*ADH2

The genome sequence of *H. volcanii* DS2 (Hartman et al. 2010) featured two putative alcohol dehydrogenase enzymes, annotated as ADH1 (HVO_2428) and ADH2 (HVO_B0071). A native expression system (Allers et al. 2010) was used for the production of *Hv*ADH1 and *Hv*ADH2. The genes *adh1* and *adh2* were cloned into the vector, pTA963, to create hexahistidine-tagged expression constructs and the proteins *Hv*ADH1 and *Hv*ADH2 were homologously overexpressed in the host *H. volcanii* strain. The expressed enzymes were soluble and active. The control supernatant, resulting from *H. volcanii* H1209 cells transformed with pTA963, was inactive, indicating that the observed activity was due to recombinant *Hv*ADH1 and *Hv*ADH2 expression. Using this expression system, the production of *Hv*ADH1 and *Hv*ADH2 proved highly efficient and fast, compared to the *H. volcanii* DS70/pRV1 expression system, previously employed for the production of an ADH from *H. marismortui* (Timpson et al. 2012).

Purification of *Hv*ADH1 and *Hv*ADH2

*Hv*ADH1 and *Hv*ADH2 were purified from *H. volcanii* H1238 and H1239 in one step by immobilized metal-affinity chromatography, using Ni^{2+} as the immobilized ion. Prior to purification, the specific activities of *Hv*ADH1 and *Hv*ADH2 with ethanol in the crude extract were approximately 0.3 and 0.2 U/mg, respectively. The His-tagged proteins eluted when 10 % (5 mM disodium EDTA) to 30 % (15 mM disodium EDTA) of elution buffer was applied. A preliminary attempt to purify the enzymes using imidazole as eluting agent resulted in a total loss of activity, an outcome that was consistent with previously documented alcohol dehydrogenase inhibition by imidazole (McKinley-McKee 1964). Several active fractions were collected and the most active fractions were pooled and analyzed by sodium dodecyl sulfate polyacrylamide gel electrophoresis (SDS-PAGE) (Fig. 1), which, in each case, revealed bands approximately corresponding to the subunit molecular weights of His-*Hv*ADH1 (37.6 kDa) (Fig. 1a) and His-*Hv*ADH2 (37.8 kDa) (Fig. 1b). The purified enzymes were subjected to dialysis to remove disodium EDTA, known to have an inhibitory effect on the activity of zinc-dependent ADHs (Vallee and Hoch 1957). Prior to dialysis, the specific activity of *Hv*ADH1 was 8.9 U/mg, indicating a purification factor of 30. Overnight dialysis resulted in a 34 % loss of activity, which proved a consistent observation following purification of *Hv*ADH1 and was attributed to inherent instability of the enzyme. By contrast, the specific activity of *Hv*ADH2 (4.8 U/mg), indicating a purification factor of 24, remained unchanged following dialysis.

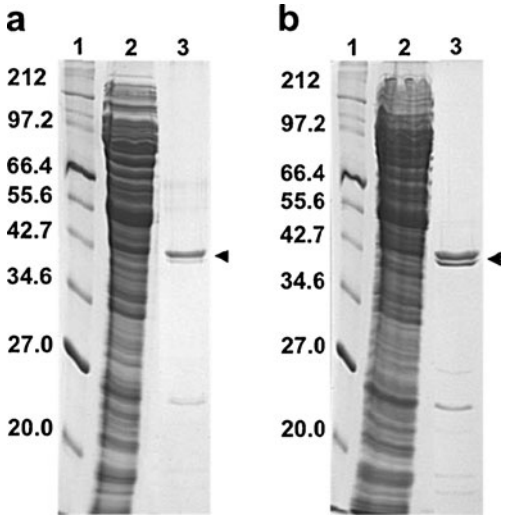

Fig. 1 SDS-PAGE visualization of **a** *Hv*ADH1 and **b** *Hv*ADH2. **a** *Lane 1* broad range protein marker P7702S; *lane 2 H. volcanii* H1238 His-*Hv*ADH1 supernatant; *lane 3* purified *Hv*ADH1. **b** *Lane 1* broad range protein marker P7702S; *lane 2 H. volcanii* H1239 His-*Hv*ADH2 supernatant; *lane 3* purified *Hv*ADH2. Molecular masses in kilodalton are indicated on the *left*. An *arrowhead* indicates the position of *Hv*ADH1 and *Hv*ADH2

Identification of *Hv*ADH1and *Hv*ADH2 by mass spectrometry

Although both proteins appeared highly pure following purification from *H. volcanii* H1238 and H1239, a second distinct band was observed directly underneath the bands designated as *Hv*ADH1 and *Hv*ADH2 (Fig. 1). In each case, both bands were excised from the gel, and resultant tryptic peptides were analyzed by ESI-Q-TOF2 tandem mass spectrometry. As expected, the protein bands designated as *Hv*ADH1 and *Hv*ADH2 were confirmed as such. Notably, peptides from both *Hv*ADH1 and *Hv*ADH2 were identified in the lower molecular mass bands. This observation sparked interest in the quaternary structures of the enzymes and raised the possibility that recombinant *Hv*ADH1 and *Hv*ADH2 were interacting with endogenous ADHs in a heterodimeric and/or heterotetrameric conformation.

Purification of *Hv*ADH1 and *Hv*ADH2 from a Δ*adh2* Δ*adh1* mutant strain

To eliminate this possibility, a Δ*adh2* Δ*adh1* double gene deletion mutant *H. volcanii* strain, H1325, was generated and transformed with pTA1202-*adh1* and with pTA1205-

adh2. *Hv*ADH1 and *Hv*ADH2 were overexpressed and purified from *H. volcanii* H1330 and *H. volcanii* H1332, respectively, according to standard procedures. Following dialysis of selected active fractions, the specific activities and purification folds of *Hv*ADH1 and *Hv*ADH2 were highly similar to those following purification and dialysis of the proteins from *H. volcanii* H1238 and H1239. SDS-PAGE visualization revealed profiles identical to those shown in Fig. 1. In each case, this consisted of an abundant upper band and a fainter lower molecular mass band, both of which were comprised solely of *Hv*ADH1 or *Hv*ADH2, according to the mass spectrometric identification data. It is likely that the lower molecular mass protein observed is a consequence of premature termination or proteolysis, a well-known phenomenon that is often reported for highly expressed recombinant proteins in *E. coli* (Baneyx and Mujacic 2004), though this is the first time that this phenomenon has been reported in *H. volcanii*. The molecular mass of the native proteins was subsequently investigated by size exclusion chromatography. When *Hv*ADH1 and *Hv*ADH2 were eluted in 2 M NaCl, the estimated molecular masses were 138 and 132 kDa, respectively, indicating tetrameric quaternary structures [theoretical values 146.9 kDa (*Hv*ADH1) and 147.9 kDa (*Hv*ADH2)]. However, when *Hv*ADH1 was eluted in 1 M NaCl, an active tetramer and a second (inactive) fraction, with a molecular mass corresponding to that of a dimer, were collected. Interestingly, the same experiment performed with *Hv*ADH2 lead to the isolation of an active dimeric form of the protein (albeit significantly less active) as well as the active tetramer. We hypothesized that the inclusion of only 1 M salt in the buffer lead to instability of the quaternary structures, resulting in dissociation of the majority of each tetramer into dimers with consequent loss of activity. To confirm this, we incubated the purified *Hv*ADH1 with 1 M NaCl at 0 °C and assayed the activity after 30 min. With respect to the enzyme incubated with 2 M NaCl under the same conditions, we noted a dramatic loss of activity of over 80 %.

Characterization of *Hv*ADH1 and *Hv*ADH2

Based on sequence alignment with experimentally validated ADHs, using the ClustalW2 program (Chenna et al. 2003), *Hv*ADH1 was predicted to be NAD^+ and *Hv*ADH2 $NADP^+$ dependent. The enzymes were subsequently experimentally screened for activity against ethanol and 1-propanol, using both coenzymes. *Hv*ADH1 was exclusively NAD^+ dependent. As predicted, *Hv*ADH2 was $NADP^+$ dependent. However, it displayed low, but significant, activity (14 % of that detected with $NADP^+$) with NAD^+ at pH 11.0 with 4 M KCl.

*Hv*ADH1 exhibited a preference for short-chain alcohol substrates, most markedly ethanol and 1-propanol (Fig. 2). Minor activity (80–90 % less than that observed with ethanol and 1-propanol) was detected against medium- and branched-chain alcohol substrates. In contrast, *Hv*ADH2 accepted a much broader range of alcohol substrates, including benzyl alcohol, and displayed a preference for medium-chain alcohols (Fig. 2).

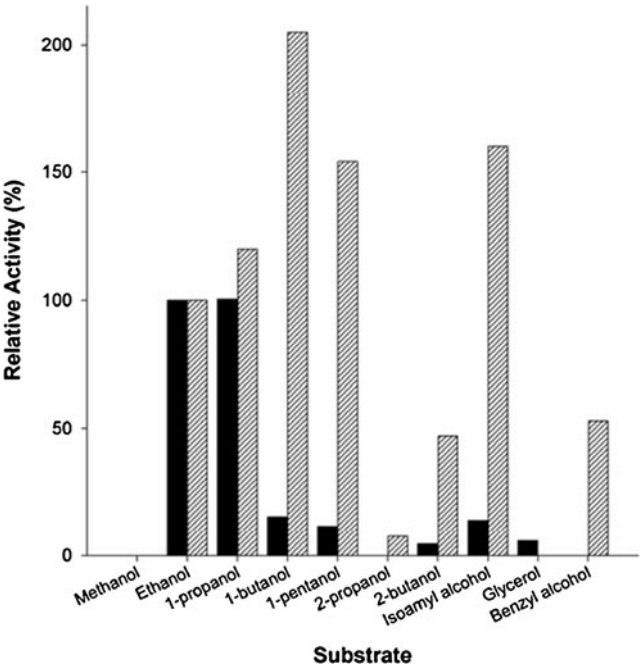

Fig. 2 *Hv*ADH1 and *Hv*ADH2 activity against a range of alcohol substrates. *Hv*ADH1 (*black bars*) and *Hv*ADH2 (*striped bars*) were assayed for activity against methanol, ethanol, 1-propanol, 1-butanol, 1-pentanol, 2-propanol, 2-butanol, isoamyl alcohol, glycerol, and benzyl alcohol. The results were expressed as relative activities (%)

As expected, both enzymes were haloalkaliphilic for the oxidative reaction and were significantly more active with KCl than with NaCl. *Hv*ADH1 was optimally active with ethanol and 1-propanol at pH 11.0 with 3 M KCl and with 1-butanol at pH 10.0 with 4 M KCl. *Hv*ADH2 catalyzed the oxidative reaction optimally at pH 10.0. Interestingly, there was an apparent negative correlation between the substrate chain length and the salt concentration required for optimum *Hv*ADH2 activity. The enzyme was maximally active with ethanol with 4 M KCl. It was maximally active with 1-propanol with 2 M KCl and with 1-butanol and 1-pentanol with 1 M KCl. Optimum *Hv*ADH2 activity with the secondary alcohols, 2-propanol and 2-butanol, was observed with 3 M KCl and 2 M KCl, respectively, and with isoamyl alcohol in the presence of 1 M KCl. Maximum activity with benzyl alcohol was detected with 2 M KCl. Both *Hv*ADH1 and *Hv*ADH2 catalyzed the reductive reaction optimally at pH 6.0, with 4 M KCl in the case of *Hv*ADH1, and with 1 M KCl in the case of *Hv*ADH2.

Both haloarchaeal enzymes described here were found to be highly thermoactive. *Hv*ADH1 exhibited maximum activity at 80 °C, while *Hv*ADH2 was maximally active between 85 and 90 °C (Fig. 3).

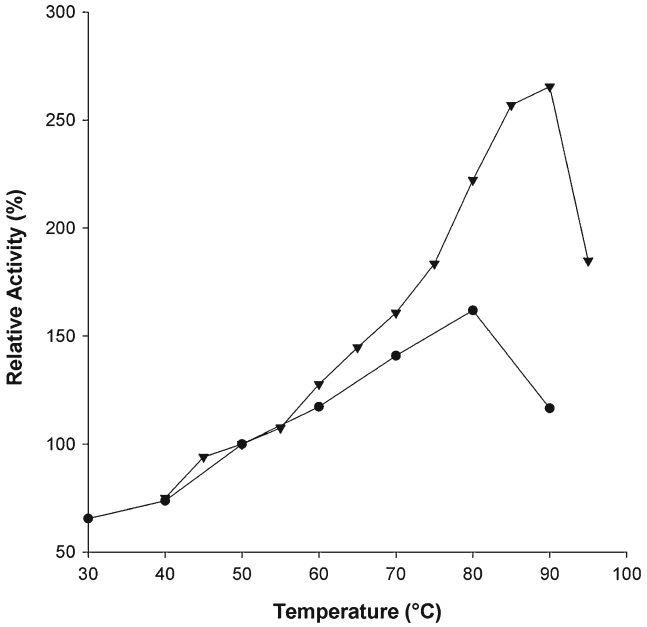

Fig. 3 Thermoactivity of *Hv*ADH1 and *Hv*ADH2. Enzyme activity of *Hv*ADH1 (*filled circle*) and *Hv*ADH2 (*filled down triangle*) was examined under standard assay conditions for the oxidative reaction at temperatures 30 °C through to 95 °C. The results were expressed as relative activities (%)

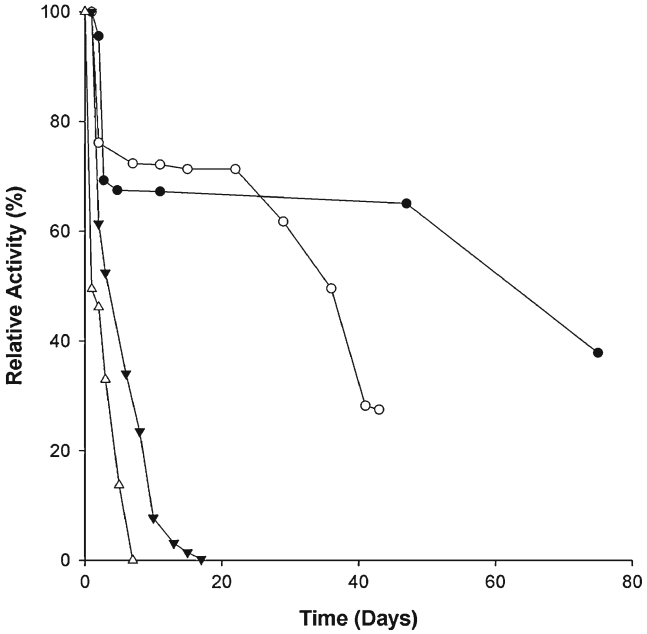

Fig. 4 Stability of *Hv*ADH1 and *Hv*ADH2. Neat *Hv*ADH1 was stored crude (*open triangle*) and following purification (*filled down triangle*) at −20 °C. Neat *Hv*ADH2 was stored crude (*filled circle*) and following purification (*open circle*) at −20 °C. The results were expressed as relative activities (%)

While the specific activity of purified *Hv*ADH1 was sufficient for subsequent characterization of the enzyme, a significant loss of activity was consistently observed following the post-purification dialysis step. To further investigate the stability of *Hv*ADH1, samples of crude and purified enzyme were stored at −20 °C with and without additives, and enzyme activity was monitored over time. Additives used in the stabilization of enzymes typically include substrates or substrate analogues, low molecular weight organic molecules and salts and sugars (Gray 1988; Schmid 1979). *Hv*ADH1 was stored neat and with ammonium sulphate (100 mM), bovine serum albumin [0.5 % (*w*/*v*)], phenylmethylsulfonyl fluoride (5 mM), and methanol [5–20 % (*v*/*v*)] (data not shown). Methanol was selected as a stabilizing additive based on the observation that *Hv*ADH1 did not accept it as a substrate. It would therefore potentially reside in the active site of the enzyme, supporting its three-dimensional structure, and reducing loss of activity due to unfavourable conformational changes. Crude and purified *Hv*ADH1 was most stable when stored neat at −20 °C (Fig. 4). However, the inherent instability of *Hv*ADH1 was apparent, with the enzyme being inactive after approximately 2 weeks. Storage at −80 °C or lyophilization (Wang 2000) of *Hv*ADH1 did not improve storage time.

With respect to *Hv*ADH1, the stability of *Hv*ADH2 was remarkable. While *Hv*ADH1 (crude and purified) was inactive after 2 weeks, crude *Hv*ADH2 retained half of its original activity following incubation at −20 °C for 75 days and purified *Hv*ADH2 retained almost one third of its original activity following incubation for 42 days (Fig. 4). Glycerol appeared to be a good stabilizing and cryoprotecting additive for the preservation of *Hv*ADH2 over a short-time period (10 days) (data not shown). However, its addition did not offer any significant advantage for the preservation of *Hv*ADH2 over longer time periods. *Hv*ADH2 was unstable when stored at 4 °C, being inactive within 10 days. The optimum pH and salt concentration for the storage of *Hv*ADH2 were investigated by incubating the enzyme in buffers varying in pH from 5.0 to 11.0 and in salt concentration from 1 to 3 M NaCl and KCl. *Hv*ADH2 was found to be most stable when stored at pH 8.0 with 2 and 3 M KCl.

In addition to its impressive stability, the tolerance of *Hv*ADH2 following overnight incubation at 4 °C with 10 and 20 % organic solvents, DMSO and ACN, was significantly greater than that reported for *Hm*ADH12, HLADH, and YADH (Timpson et al. 2012) (Table 1). *Hv*ADH2 was subsequently incubated for a longer period of time (72 h) at 4 °C with 5, 10, and 30 % (*v*/*v*) DMSO, ACN, and methanol. Following incubation with 5 and 10 % DMSO, *Hv*ADH2 retained 74 and 69 % activity, respectively. The enzyme retained 65 and 63 % activity following incubation with 5 and 10 % ACN, respectively. Finally, *Hv*ADH2 retained 70 and 67 % activity following incubation with 5 and 10 % methanol, respectively. Upon increasing the solvent concentration to 30 %, *Hv*ADH2 still retained 47 and 39 % activity following incubation with DMSO and methanol, respectively, while it was completely inactivated following 72 h incubation with 30 % ACN.

Table 1 Effect of solvents on *Hv*ADH2, HLADH, and YADH activity over 24 h at 4 °C

	Residual activity (%)		
	*Hv*ADH2	HLADH	YADH
10 % DMSO	85	10	72
20 % DMSO	85	7	–
10 % ACN	87	73	39
20 % ACN	18	0	–
10 % Tetrahydrofuran	3	0	0

*Hv*ADH1 followed Michaelis–Menten kinetics, and the kinetic parameters of *Hv*ADH1 for substrates and coenzymes of the oxidative and reductive reactions were comparable (Table 2). The quick inactivation of the enzyme may contribute to the observed differences in the reported V_{max} values. *Hv*ADH2 displayed positive cooperativity in the oxidative reaction, with Hill coefficient values of 1.62± 0.05 for ethanol and 1.9±0.2 for 1-butanol. Kinetic experiments confirmed that *Hv*ADH2 preferentially accepted 1-butanol as a substrate over ethanol in the oxidative reaction. The enzyme appeared to follow Michaelis–Menten kinetics with the coenzymes $NADP^+$ and NADPH and with acetaldehyde (Table 2).

Discussion

There is considerable interest in haloarchaeal alcohol dehydrogenases due to their potential application in industrial processes. The fact that haloarchaeal enzymes often exhibit intrinsic tolerance to organic solvents makes them an exciting option for reactions that must be performed using organic media. For biotechnological application, it is desirable that a given haloarchaeal ADH exhibit broad substrate specificity, NAD^+ dependence, stability and an ability to withstand organic cosolvents, and high temperatures. In this study, we investigated two novel alcohol dehydrogenases from *H. volcanii* for this purpose.

His-tagged *Hv*ADH1 and *Hv*ADH2 were cloned, homologously overexpressed and purified from *H. volcanii* strains. The production of *Hv*ADH1 and *Hv*ADH2 was highly efficient due to the selection of transformed *H. volcanii* cells by *pyr*E2 and *hdr*B markers, which maintain plasmids in rich medium without the requirement for antibiotics, known to impair cell growth (Allers et al. 2010). Both enzymes were soluble and exhibited alcohol dehydrogenase activity that was approximately 10-fold greater than that previously reported for ADH12 from *H. marismortui* (Timpson et al. 2012).

*Hv*ADH1 and *Hv*ADH2 featured key conserved Cys and His residues involved in the binding of catalytic zinc and the quartet of Cys residues involved in structural zinc binding. Like other haloarchaeal enzymes, *Hv*ADH1 and *Hv*ADH2 featured an excess of acidic residues, a feature of molecular adaptation to high intracellular KCl concentrations (Coquelle et al. 2010). In contrast to the mesophilic HLADH, the amino acid sequence of which features 10 % acidic residues, the sequences for *Hv*ADH1 and *Hv*ADH2 feature 15 and 17 % acidic residues, respectively, figures in agreement with those reported for other haloarchaeal enzymes (Camacho et al. 2002; Cao et al. 2008a). The coenzyme binding domain in ADHs is highly conserved and is known as the Rossmann fold. Residues located at the C-terminal end of the second β-strand of the nucleotide-binding βαβ motif are considered determinants of coenzyme dependency (Pire et al. 2009). NAD^+-dependent dehydrogenases generally feature a highly, but not absolutely, conserved negatively charged Asp or Glu residue at this position whereas $NADP^+$-dependent dehydrogenases often feature a corresponding Gly or Arg residue (Lesk 1995; Wierenga et al. 1985). *Hv*ADH1 featured an Asp residue at this position and was, as predicted, exclusively NAD^+ dependent, a highly attractive attribute of the enzyme as it removes any requirement to shift the cofactor dependency of the enzyme for economic reasons in the future. *Hv*ADH2, in contrast, featured a Gly residue and displayed a strong preference for the phosphorylated coenzyme. However, if necessary, *Hv*ADH2 could be engineered to principally accommodate NAD^+, or, alternatively, coenzyme regeneration could be employed to counter the coenzyme expense.

Table 2 Kinetic parameters of *Hv*ADH1 and *Hv*ADH2

	*Hv*ADH1			*Hv*ADH2		
Substrate/cofactor	K_m (mM)	V_{max} (μmol min^{-1} mg^{-1})	K_{cat}/K_m (s^{-1} mM^{-1})	K_m (mM)	V_{max} (μmol min^{-1} mg^{-1})	K_{cat}/K_m (s^{-1} mM^{-1})
Ethanol	31±2	3.65±0.08	0.072	44±1 ($K_{0.5}$)	5.01±0.07	0.070 ($K_{cat}/K_{0.5}$)
1-Butanol	–	–	–	6.7±0.2 ($K_{0.5}$)	5.2±0.1	0.479 ($K_{cat}/K_{0.5}$)
Acetaldehyde	28±3	2.2±0.1	0.048	9.2±0.9	11.1±0.3	0.744
$NAD(P)^+$	0.29±0.02	4.28±0.08	9.037	0.21±0.01	4.22±0.09	12.390
NAD(P)H	0.071±0.008	3.8±0.2	32.771	0.032±0.002	12.6±0.4	242.763

Both *Hv*ADH1 and *Hv*ADH2 were halophilic, and this was confirmed by the apparent dissociation of *Hv*ADH1 and *Hv*ADH2 tetramers into less active dimers, when eluted in 1 M NaCl. This result is consistent with the defining feature of protein halophilicity, that being the rapid dissociation and loss of enzyme activity at salt concentrations below 1 M, coupled with the requirement of such enzymes for molar concentrations of salt for optimum activity (Sellek and Chaudhuri 1999).

Importantly, *Hv*ADH2 accepted a broad range of substrates, with most marked activity detected with the medium-chain alcohols 1-butanol and 1-pentanol. Interestingly, the enzyme was also active with the branched-chain substrate isoamyl alcohol and the aromatic substrate benzyl alcohol. Conversely, *Hv*ADH1 primarily accepted ethanol and 1-propanol, with only minor activity detected with medium and branched-chain substrates.

It is well known that haloarchaeal enzymes are not only halophilic, but are often also thermoactive (Cao et al. 2008a,b), an observation that has been ascribed to shared structural features, which contribute to the stability of both haloarchaeal and thermoarchaeal enzymes (Dym et al. 1995). The thermoactivity of both *Hv*ADH1 and *Hv*ADH2 was impressive and *Hv*ADH2, in particular, is the most thermoactive haloarchaeal ADH of those reported to date (Cao et al. 2008a; Timpson et al. 2012). Given the importance of biocatalyst stability under process conditions, the practical applicability of *Hv*ADH1, and particularly *Hv*ADH2, is strengthened by both their halophilicity and high degree of thermoactivity (Huisman et al. 2010).

*Hv*ADH1 and *Hv*ADH2 contrasted dramatically in terms of their stability. *Hv*ADH2 was remarkably stable when stored both neat and when stored with glycerol at −20 °C. Although mutagenic approaches towards enhancing the stability of *Hv*ADH1 could increase the viability of its potential industrial application, its current application is severely limited due to its poor stability. As well as being intrinsically stable, *Hv*ADH2 also tolerated organic solvents ACN and DMSO at concentrations of 10 and 20 %, respectively. The data obtained following incubation of *Hv*ADH2 for 72 h with DMSO, ACN, and methanol further highlight the stability of *Hv*ADH2. This, together with its activity, broad substrate specificity, halophilicity, and thermoactivity, makes *Hv*ADH2 a far more attractive choice of enzyme to proceed with in the future.

This study represents the first report on alcohol dehydrogenases from *H. volcanii*. Through this research, we have demonstrated the efficient and consistent production of new, promising extremozymes with potential biotechnological applications. The information gathered from this work has allowed for the comparison of *Hv*ADH1 and *Hv*ADH2 with a view to assessing their potential biotechnological application. While the industrial potential of *Hv*ADH1 is restricted due to its instability, *Hv*ADH2 appears to be an extremely promising enzyme. Our research contributes to the progression of biocatalyst discovery and provides a robust platform from which *Hv*ADH2 may be further developed for practical biotechnological application.

Acknowledgments This work was supported by a research grant awarded to F.P. by Science Foundation Ireland (SFI), a University Research Fellowship awarded to T.A. by the Royal Society, and funding provided by the Islamic Development Bank (IsDB).

References

Adams MWW, Perler FB, Kelly RM (1995) Extremozymes: expanding the limits of biocatalysis. Nat Biotechnol 13:662–668

Allers T, Ngo HP, Mevarech M, Lloyd RG (2004) Development of additional selectable markers for the halophilic archaeon *Haloferax volcanii* based on the *leuB* and *trpA* genes. Appl Environ Microbiol 70:943–953

Allers T, Barak S, Liddell S, Wardell K, Mevarech M (2010) Improved strains and plasmid vectors for conditional overexpression of his-tagged proteins in *Haloferax volcanii*. Appl Environ Microbiol 76:1759–1769

Baneyx F (1999) Recombinant protein expression in *Escherichia coli*. Curr Opin Biotechnol 10:411–421

Baneyx F, Mujacic M (2004) Recombinant protein folding and misfolding in *Escherichia coli*. Nat Biotechnol 22:1399–1408

Bitan-Banin G, Ortenberg R, Mevarech M (2003) Development of a gene knockout system for the halophilic archaeon *Haloferax volcanii* by use of the *pyrE* gene. J Bacteriol 185:772–778

Camacho M, Rodriguez-Arnedo A, Bonete M (2002) NADP-dependent isocitrate dehydrogenase from the halophilic archaeon *Haloferax volcanii*: cloning, sequence determination and overexpression in *Escherichia coli*. FEMS Microbiol Lett 209:155–160

Cao Y, Liao L, Xu X, Oren A, Wang C, Zhu X, Wu M (2008a) Characterization of alcohol dehydrogenase from the haloalkaliphilic archaeon *Natronomonas pharaonis*. Extremophiles 12:471–476

Cao Y, Liao L, Xu X, Oren A, Wu M (2008b) Aldehyde dehydrogenase of the haloalkaliphilic archaeon *Natronomonas pharaonis* and its function in ethanol metabolism. Extremophiles 12:849–854

Cendrin F, Chroboczek J, Zaccai G, Eisenberg H, Mevarech M (1993) Cloning, sequencing, and expression in *Escherichia coli* of the gene coding for malate dehydrogenase of the extremely halophilic archaebacterium *Haloarcula marismortui*. Biochemistry 32:4308–4313

Chenna R, Sugawara H, Koike T, Lopez R, Gibson TJ, Higgins DG, Thompson JD (2003) Multiple sequence alignment with the Clustal series of programs. Nucleic Acids Res 31:3497–3500

Connaris H, Chaudhuri JB, Danson MJ, Hough DW (1999) Expression, reactivation, and purification of enzymes from *Haloferax volcanii* in *Escherichia coli*. Biotechnol Bioeng 64:38–45

Coquelle N, Talon R, Juers DH, Girard E, Kahn R, Madern D (2010) Gradual adaptive changes of a protein facing high salt concentrations. J Mol Biol 404:493–505

Danson MJ, Hough DW (1998) Structure, function and stability of enzymes from the Archaea. Trends Microbiol Rev 6:307–314

Dym O, Mevarech M, Sussman JL (1995) Structural features that stabilize halophilic malate dehydrogenase from an archaebacterium. Science 267:1344–1346

Eichler J (2001) Biotechnological uses of archaeal extremozymes. Biotechnol Adv 19:261–278

Flam F (1994) The chemistry of life at the margins. Science 265:471–472

Friest JA, Maezato Y, Broussy S, Blum P, Berkowitz DB (2010) Use of a robust dehydrogenase from an archael hyperthermophile in asymmetric catalysis-dynamic reductive kinetic resolution entry into (S)-profens. J Am Chem Soc Commun 132:5930–5931

Giacomini D, Galletti P, Quintavalla A, Gucciardo G, Paradisi F (2007) Highly efficient asymmetric reduction of arylpropionic aldehydes by horse liver alcohol dehydrogenase through dynamic kinetic resolution. Chem Commun 21:4038–4040

Goldberg K, Schroer K, Lütz S, Liese A (2007) Biocatalytic ketone reduction—a powerful tool for the production of chiral alcohols—part I: processes with isolated enzymes. Appl Microbiol Biotechnol 76:237–248

Gray CJ (1988) Additives and enzyme stability. Biocatal Biotrans 1:187–196

Guy CP, Haldenby S, Brindley A, Walsh DA, Briggs GS, Warren MJ, Allers T, Bolt EL (2006) Interactions of RadB, a DNA repair protein in archaea, with DNA and ATP. J Mol Biol 358:46–56

Hartman AL, Norais C, Badger JH, Delmas S, Haldenby S, Madupu R, Robinson J, Khouri H, Ren Q, Lowe TM, Maupin-Furlow J, Pohlschroder M, Daniels C, Pfeiffer F, Allers T, Eisen JA (2010) The complete genome sequence of *Haloferax volcanii* DS2, a model archaeon. PLoS One 5:e9605

Hough DW, Danson MJ (1999) Extremozymes. Curr Opin Chem Biol 3:39–46

Huisman GW, Liang J, Krebber A (2010) Practical chiral alcohol manufacture using ketoreductases. Curr Opin Chem Biol 14:122–129

Lesk AM (1995) NAD-binding domains of dehydrogenases. Curr Opin Struct Biol 5:775–783

McKinley-McKee J (1964) The mechanism of action and the active centre of the alcohol dehydrogenases. Progr Biophys Mol Biol 14:225–262

Norais C, Hawkins M, Hartman AL, Eisen JA, Myllykallio H, Allers T (2007) Genetic and physical mapping of DNA replication origins in *Haloferax volcanii*. PLoS Genet 3:e77

Oren A (2002) Diversity of halophilic microorganisms: environments, phylogeny, physiology, and applications. J Ind Microbiol Biotechnol 28:56–63

Parkot J, Gröger H, Hummel W (2010) Purification, cloning, and overexpression of an alcohol dehydrogenase from *Nocardia globerula* reducing aliphatic ketones and bulky ketoesters. Appl Microbiol Biotechnol 86:1813–1820

Pire C, Esclapez J, Diaz S, Perez-Pomares F, Ferrer J, Bonete MJ (2009) Alteration of coenzyme specificity in halophilic NAD $(P)^+$ glucose dehydrogenase by site-directed mutagenesis. J Mol Catal B: Enzym 59:261–265

Schmid RD (1979) Stabilized soluble enzymes. Adv Biochem Eng Biotechnol 12:41–118

Sellek GA, Chaudhuri JB (1999) Biocatalysis in organic media using enzymes from extremophiles. Enzyme Microb Technol 25:471–482

Singh SM, Panda AK (2005) Solubilization and refolding of bacterial inclusion body proteins. J Biosci Bioeng 99:303–310

Timpson LM, Alsafadi D, Mac Donnchadha C, Liddell S, Sharkey MA, Paradisi F (2012) Characterization of alcohol dehydrogenase (ADH12) from *Haloarcula marismortui*, an extreme halophile from the Dead Sea. Extremophiles 16:57–66

Vallee BL, Hoch FL (1957) Zinc in horse liver alcohol dehydrogenase. J Biol Chem 225:185–195

Wang W (2000) Lyophilization and development of solid protein pharmaceuticals. Int J Pharm 203:1–60

Wierenga RK, De Maeyer MCH, Hol WGJ (1985) Interaction of pyrophosphate moieties with alpha-helixes in dinucleotide-binding proteins. Biochemistry 24:1346–1357

Wilkinson GN (1961) Statistical estimations in enzyme kinetics. Biochem J 80:324–332

Yakushi T, Matsushita K (2010) Alcohol dehydrogenase of acetic acid bacteria: structure, mode of action, and applications in biotechnology. Appl Microbiol Biotechnol 86:1257–1265